A hyperbolic model for convection-diffusion transport problems in CFD: Numerical analysis and applications

Héctor Gómez, Ignasi Colominas *, Fermín Navarrina and Manuel Casteleiro

Group of Numerical Methods in Engineering, GMNI
Dept. of Applied Mathematics, School of Civil Engineering
Universidad de A Coruña
Campus de Elviña, 15071 A Coruña, Spain

Abstract

In this paper we present a numerical study of a hyperbolic model for convection-diffusion transport problems that has been recently proposed by the authors [1]. This model avoids the infinite speed paradox, inherent to the standard parabolic model and introduces a new parameter τ called relaxation time. This parameter plays the role of an "inertia" for the movement of the pollutant.

The analysis presented herein is twofold: firstly, we perform an accurate study of the 1D steady equations and its numerical solution. We compare the solution of the hyperbolic model with that of the parabolic model and we analyze the influence of the relaxation time on the solution. On the other hand, we explore the possibilities of the proposed model for real computations in engineering. With this aim we solve an example concerning the evolution of a pollutant being spilled in the harbor of A Coruña (northwest of SPAIN, EU).

Key words: Convection-Diffusion, Cattaneo's equation, Finite velocity.

* Correspondence to: E.T.S. de Ingenieros de Caminos, Canales y Puertos, Universidad de A Coruña, Campus de Elviña, 15071 A Coruña, Spain.
Email address: icolominas@udc.es (Ignasi Colominas).

1 Introduction

There is much experimental evidence which proves that diffusive processes take place with finite velocity inside matter [2,3]. However, standard parabolic models based on Fick's law [4] or Fourier's law [5] (in the case of mass transport or heat conduction respectively) predict an infinite speed of propagation. In some applications, this issue can be ignored and the use of parabolic models is assumed to be accurate enough for practical purposes in spite of predicting an infinite speed of propagation [6]. However, in many other applications it is necessary to take into account the wave nature of diffusive processes to perform accurate predictions [2,7]. This kind of approach cannot be carried out by using Fick's law or Fourier's law. Instead a more general constitutive law, for example the one proposed by Cattaneo [6], must be employed.

In the past, the study of the hyperbolic diffusion has been limited to pure-diffusive problems [8–11]. Recently the authors have proposed a generalization of the hyperbolic diffusion equation that can also be used in convective cases [12–14]. From a numerical point of view, the simulation of the hyperbolic diffusion equation has been mostly limited to 1D problems [15,16]. The numerical discretization of 2D pure-diffusion problems was probably pioneered by Yang [17]. Later, Manzari et al. [18] proposed a different algorithm and solved some practical pure-diffusive examples.

The first objective of this paper is to perform an accurate analysis of the 1D steady convection-diffusion equation and its numerical solution. We compare the parabolic and the hyperbolic models by means of their numerical and exact solutions. The objective is to analyze whether the infinite speed paradox (inherent to the parabolic model) contributes or not to the numerical instabilities that appear in convection dominated flows discretized with centered methods. The fact is that there is a well-known example that may be related to the one presented herein. In the context of CFD, the assumption of incompressibility leads to the result that pressure waves can travel at an infinite speed. The velocity of pressure waves becomes finite when one removes this assumption and many of the problems that appear in the numerical resolution of incompressible flow problems do not appear in compressible fluid computations.

The second objective of this paper is to explore the possibilities of the hyperbolic model for practical computations in engineering in the context of mass diffusion within a fluid. In this framework, there are a lot of important applications in civil and environmental engineering, for instance, the prediction of the fate of a pollutant spilled in a fluid. This paper presents an example concerning the evolution of a pollutant being spilled in the harbor of A Coruña (northwest of SPAIN, EU).

The outline of this paper is as follows: In Section 2 we review the parabolic formulation of the convective-diffusive equation. In section 3 we present the hyperbolic model for the transport problem. A numerical analysis of the 1D steady state equations is performed in section 4. In section 5 we solve a practical case in environmental engineering. Finally, section 6 is devoted to the presentation of the main conclusions of this study.

2 Standard formulation of the convection-diffusion transport problem

In this section we review the classic formulation for the convection-diffusion transport problem. We assume the medium to be incompressible and we do not consider source terms. The governing equations under these hypotheses are as follows:

$$\frac{\partial u}{\partial t} + \boldsymbol{a} \cdot \nabla_{\boldsymbol{x}} (u) + \nabla_{\boldsymbol{x}} \cdot (\boldsymbol{q}) = 0 \tag{1.1}$$

$$\boldsymbol{q} = -\boldsymbol{K} \nabla_{\boldsymbol{x}} (u) \tag{1.2}$$

In the above system, (1.1) is the mass conservation equation and (1.2) is the constitutive equation known as Fick's law. Furthermore, u is the pollutant concentration, $\boldsymbol{a}$ is the velocity field which satisfies the hydrodynamic equations of an incompressible fluid, $\boldsymbol{q}$ is the diffusive flux per unit fluid density and $\boldsymbol{K}$ is the diffusivity tensor which is assumed to be positive definite. Clearly, system (1) can be decoupled since we can introduce (1.2) into (1.1) and solve the scalar equation

$$\frac{\partial u}{\partial t} + \boldsymbol{a} \cdot \nabla_{\boldsymbol{x}} (u) - \nabla_{\boldsymbol{x}} \cdot (\boldsymbol{K} \nabla_{\boldsymbol{x}} (u)) = 0 \tag{2}$$

It is well known that equation (2) is parabolic. Therefore, boundary conditions must be imposed everywhere on the boundary of the domain [20]. Then, let us consider the transport by convection and diffusion in a domain $\Omega \subset \mathbb{R}^2$ with piecewise smooth boundary Γ. The unit outward normal vector to Γ is denoted by $\boldsymbol{n}$. The boundary is assumed to consist of a portion Γ_D on which the value of u is prescribed (Dirichlet or essential conditions) and a complementary portion Γ_N on which flux is prescribed (Neumann or natural conditions). In addition, we know the initial distribution of the transported quantity u. At this point we can state convection-diffusion initial-boundary value problem as follows: given a divergence free velocity field $\boldsymbol{a}$, given the diffusion tensor $\boldsymbol{K}$ and given adequate initial and boundary conditions, find $u \colon \Omega \times [0, T] \mapsto \mathbb{R}$

such that

$$\frac{\partial u}{\partial t} + \boldsymbol{a} \cdot \nabla_{\boldsymbol{x}} (u) - \nabla_{\boldsymbol{x}} \cdot (\boldsymbol{K} \nabla_{\boldsymbol{x}} (u)) = 0 \qquad \text{in} \quad \Omega \times [0, T] \tag{3.1}$$

$$u(\boldsymbol{x}, 0) = u_0(\boldsymbol{x}) \qquad \text{on} \quad \Omega \tag{3.2}$$

$$u = u_D \qquad \text{on} \quad \Gamma_D \times (0, T] \tag{3.3}$$

$$\boldsymbol{K} \nabla_{\boldsymbol{x}} (u) \cdot \boldsymbol{n} = h \qquad \text{on} \quad \Gamma_N \times (0, T] \tag{3.4}$$

3 A hyperbolic model for convection-diffusion problems

3.1 Governing equations

The hyperbolic model for convection-diffusion problems is obtained by substituting Fick's law (equation (1.2)) by a more general equation based on Cattaneo's law. Cattaneo's equation was originally proposed for non-advective problems and it can not be used directly for convection-diffusion problems. For this reason the authors have recently proposed [12–14] the following constitutive equation:

$$\boldsymbol{q} + \boldsymbol{\tau} \left(\frac{\partial \boldsymbol{q}}{\partial t} + \nabla_{\boldsymbol{x}} (\boldsymbol{q}) \, \boldsymbol{a} \right) = -\boldsymbol{K} \nabla_{\boldsymbol{x}} (u) \tag{4}$$

which can be used when the medium is moving with velocity $\boldsymbol{a}$. Equation (4) has been derived from Cattaneo's law by imposing Galilean invariance principle to the resulting model. In this way, the description of the diffusion process is granted to be the same in every inertial frame [19].

Equation (4) can be closed by using the mass conservation equation. To derive the mass conservation equation we will suppose the medium to be incompressible and we will not consider source terms. In this way, the governing equations are as follows:

$$\frac{\partial u}{\partial t} + \boldsymbol{a} \cdot \nabla_{\boldsymbol{x}} (u) + \nabla_{\boldsymbol{x}} \cdot (\boldsymbol{q}) = 0 \tag{5.1}$$

$$\boldsymbol{q} + \boldsymbol{\tau} \left(\frac{\partial \boldsymbol{q}}{\partial t} + \nabla_{\boldsymbol{x}} (\boldsymbol{q}) \, \boldsymbol{a} \right) = -\boldsymbol{K} \nabla_{\boldsymbol{x}} (u) \tag{5.2}$$

It should be noted that system (5) constitutes a generalization of the classic parabolic convection-diffusion model since we can recover the standard formulation by setting $\boldsymbol{\tau} = 0$.

3.2 Conservative form

System (5) can be written as one single second order partial differential equation when the velocity field is constant; otherwise, it must be solved as a coupled system of first order partial differential equations [12].

If we introduce the hypothesis that $\boldsymbol{\tau}$ is a regular matrix (this appears to be reasonable; in fact, it seems natural to demand $\boldsymbol{\tau}$ to be positive-definite since it is somehow representing a characteristic time of the diffusion process) and we use again that the fluid medium is incompressible, system (5) can be written as a system of conservation laws as follows:

$$\frac{\partial u}{\partial t} + \nabla_{\boldsymbol{x}} \cdot (u\boldsymbol{a} + \boldsymbol{q}) = 0 \tag{6.1}$$

$$\frac{\partial \boldsymbol{q}}{\partial t} + \nabla_{\boldsymbol{x}} \cdot (\boldsymbol{q} \otimes \boldsymbol{a} + \boldsymbol{\tau}^{-1}\boldsymbol{K}u) = u\nabla_{\boldsymbol{x}} \cdot (\boldsymbol{\tau}^{-1}\boldsymbol{K}) - \boldsymbol{\tau}^{-1}\boldsymbol{q} \tag{6.2}$$

For the sake of simplicity we will consider from here on the medium to be homogeneous and isotropic (hence, $\boldsymbol{K} = k\boldsymbol{I}$, $\boldsymbol{\tau} = \tau\boldsymbol{I}$ for certain $k, \tau \in \mathbb{R}^+$). Under these hypotheses, system (6) can be written as

$$\frac{\partial u}{\partial t} + \nabla_{\boldsymbol{x}} \cdot (u\boldsymbol{a} + \boldsymbol{q}) = 0 \tag{7.1}$$

$$\frac{\partial (\tau\boldsymbol{q})}{\partial t} + \nabla_{\boldsymbol{x}} \cdot (\tau\boldsymbol{q} \otimes \boldsymbol{a} + ku\boldsymbol{I}) + \boldsymbol{q} = 0 \tag{7.2}$$

In what follows one and two-dimensional problems will be studied separately.

3.2.1 One-dimensional problem

In this section we will study the one-dimensional Cattaneo-type transport problem. In this simple case the governing equation is

$$\frac{\partial \boldsymbol{U}}{\partial t} + \nabla_{\boldsymbol{x}} \cdot (\boldsymbol{F}) = \boldsymbol{S} \tag{8}$$

where

$$\boldsymbol{U} = \begin{pmatrix} u \\ \tau q \end{pmatrix}; \quad \boldsymbol{F} = \begin{pmatrix} ua + q \\ \tau q a + ku \end{pmatrix}; \quad \boldsymbol{S} = \begin{pmatrix} 0 \\ -q \end{pmatrix} \tag{9}$$

System (8) can be written in a non-conservative form as

$$\frac{\partial \boldsymbol{U}}{\partial t} + \boldsymbol{A}\frac{\partial \boldsymbol{U}}{\partial x} = \boldsymbol{S} \tag{10}$$

being $\boldsymbol{A}$ the so-called Jacobian matrix defined by

$$\boldsymbol{A} = \nabla_{\boldsymbol{U}} (\boldsymbol{F}) = \begin{pmatrix} a & 1/\tau \\ k & a \end{pmatrix} \tag{11}$$

It is well known (see for instance reference [20]) that system (8) will be totally hyperbolic if, and only if, matrix $\boldsymbol{A}$ yields 2 different real eigenvalues. It can be shown that

$$\boldsymbol{A} = \boldsymbol{C}\boldsymbol{D}\boldsymbol{C}^{-1} \quad \text{where} \quad \boldsymbol{C} = \begin{pmatrix} 1 & 1 \\ \tau c & -\tau c \end{pmatrix}; \quad \boldsymbol{D} = \begin{pmatrix} a+c & 0 \\ 0 & a-c \end{pmatrix} \tag{12}$$

being

$$c = \sqrt{k/\tau} \tag{13}$$

the celerity of the pollutant wave.

As a consequence, system (8) is totally hyperbolic. Now we will prove that system (10) can be diagonalized but it can not be decoupled. The so-called Riemann quasi-invariants can be defined (we call Riemann quasi-invariants those functions instead of Riemann invariants [20] because there is a source term in (8)). To prove this fact, we use (12). Hence, we can rewrite (10) as follows:

$$\frac{\partial \boldsymbol{U}}{\partial t} + \boldsymbol{C}\boldsymbol{D}\boldsymbol{C}^{-1}\frac{\partial \boldsymbol{U}}{\partial x} = \boldsymbol{S} \tag{14}$$

As a consequence of the assumption of homogeneity, (14) takes the form

$$\frac{\partial (\boldsymbol{C}^{-1}\boldsymbol{U})}{\partial t} + \boldsymbol{D}\frac{\partial (\boldsymbol{C}^{-1}\boldsymbol{U})}{\partial x} = \boldsymbol{C}^{-1}\boldsymbol{S} \tag{15}$$

If we use the notation

$$\begin{pmatrix} R_1 \\ R_2 \end{pmatrix} = \boldsymbol{R} = \boldsymbol{C}^{-1}\boldsymbol{U} = \frac{1}{2}\begin{pmatrix} u + q/c \\ u - q/c \end{pmatrix} \tag{16}$$

for Riemann quasi-invariants the following equation holds:

$$\frac{\partial \boldsymbol{R}}{\partial t} + \boldsymbol{D}\frac{\partial \boldsymbol{R}}{\partial x} = \boldsymbol{Q}\boldsymbol{R} \tag{17}$$

where $\boldsymbol{Q}$ is the matrix

$$\boldsymbol{Q} = \frac{1}{2\tau}\begin{pmatrix} -1 & 1 \\ 1 & -1 \end{pmatrix} \tag{18}$$

Therefore, since $\boldsymbol{D}$ is a diagonal matrix (and $\boldsymbol{Q}$ is not a diagonal one), system (17) is only coupled by the source term. The two scalar equations in (17) are

two transport equations with a source term. The quantity R_1 is transported along the spatial coordinate with velocity $a + c$. Whereas, R_2 is also transported along the spatial coordinate in this case with velocity $a - c$. Hence, the direction in which each wave R_1 or R_2 is transported along the spatial coordinate depends on the sign of its corresponding velocity of propagation. Therefore, depending on the values of a and c the solution of (17) can be the superposition of two waves traveling in the same or in the opposite direction. We will refer to this situation as *supercritical* and *subcritical flow* respectively. At this point it is useful to introduce the following dimensionless number:

$$H = \frac{|a|}{c} \tag{19}$$

This number plays a similar role to Mach number in compressible flow problems [21] or Froude number in shallow water problems [22]. By using this dimensionless number we can differentiate three kinds of flow

- $H < 1 \Leftrightarrow$ Subcritical flow
- $H > 1 \Leftrightarrow$ Supercritical flow
- $H = 1 \Leftrightarrow$ Critical flow

Taking into account all of this, boundary conditions which should be imposed to (17) are straightforward. Let us suppose that we have to solve (17) in a given domain $\Omega = (0, L);\ \ L \in \mathbb{R}^+$ which is bounded by Γ. We will call *inflow boundary* (Γ^{in} in what follows) the part of the boundary in which $\boldsymbol{a} \cdot \boldsymbol{n} < 0$. We will call *outflow boundary* (Γ^{out} in short) the complementary part of the boundary. Now, we define Γ_0 as the point $x = 0$ and Γ_L as $x = L$. Accordingly, $\Gamma = \Gamma_0 \cup \Gamma_L$. In supercritical flow both R_1 and R_2 should be prescribed in the inflow boundary (Γ_0 when $a > 0$ and Γ_L when $a < 0$). If the flow is subcritical the quantity R_1 should be prescribed in Γ_0 and R_2 must be imposed in Γ_L .

However, it is commonly accepted [23] that a hyperbolic system of partial differential equations like (8) is well-posed when the number of imposed components of $\boldsymbol{U}$ on one boundary equals the number of negative eigenvalues of the jacobian matrix. Therefore, in supercritical flow conditions both components of $\boldsymbol{U}$ should be prescribed on the inflow boundary and no components of $\boldsymbol{U}$ must be imposed on the outflow boundary. In subcritical flow one component of $\boldsymbol{U}$ should be prescribed on the inflow boundary and the other one must be imposed on the outflow boundary. In what follows, components of $\boldsymbol{U}$ prescribed on the boundary will be called *inflow components of* $\boldsymbol{U}$. These functions will be denoted as $\boldsymbol{U}^{\text{in}}$. Therefore, the one-dimensional Cattaneo-type transport problem can be stated as follows: given $k, \tau > 0$, given the field velocity a and given adequate initial and boundary conditions,

find $\boldsymbol{U}\colon \Omega \times [0,T] \mapsto \mathbb{R}^2$ such that

$$\frac{\partial \boldsymbol{U}}{\partial t} + \nabla_{\boldsymbol{x}} \cdot (\boldsymbol{F}) = \boldsymbol{S} \qquad \text{in} \quad \Omega \times [0,T] \tag{20.1}$$

$$\boldsymbol{U}(x,0) = \boldsymbol{U}_0(x) \qquad \text{on} \quad \Omega \tag{20.2}$$

$$\boldsymbol{U}^{\text{in}} = \boldsymbol{U}_D^{\text{in}} \qquad \text{on} \quad \Gamma \times [0,T] \tag{20.3}$$

being $\boldsymbol{U}$, $\boldsymbol{F}$ and $\boldsymbol{S}$ the vectors defined in (9).

3.2.2 Two-dimensional problem

The 2D counterpart of the study presented in section 3.2.1 can be found in [1,24]. We only present herein the conservative form of the equations:

$$\frac{\partial \boldsymbol{U}}{\partial t} + \nabla_{\boldsymbol{x}} \cdot (\boldsymbol{F}) = \boldsymbol{S} \tag{21}$$

where

$$\boldsymbol{U} = \begin{pmatrix} u \\ \tau q_1 \\ \tau q_2 \end{pmatrix}; \quad \boldsymbol{F} = \begin{pmatrix} ua_1 + q_1 & ua_2 + q_2 \\ \tau q_1 a_1 + ku & \tau q_1 a_2 \\ \tau q_2 a_1 & \tau q_2 a_2 + ku \end{pmatrix}; \quad \boldsymbol{S} = \begin{pmatrix} 0 \\ -q_1 \\ -q_2 \end{pmatrix} \tag{22}$$

Note that we have used the notation $\boldsymbol{q} = (q_1, q_2)^T$ and $\boldsymbol{a} = (a_1, a_2)^T$.

4 Numerical analysis of the 1D steady state Cattaneo-type convection-diffusion equations

4.1 The negative diffusion introduced by Cattaneo's law

In this section we will show that Cattaneo's law introduces a negative diffusion with respect to Fick's law. The governing equations in this case are:

$$\nabla_{\boldsymbol{x}} \cdot (\boldsymbol{F}) = \boldsymbol{S} \tag{23}$$

being $\boldsymbol{F}$ and $\boldsymbol{S}$ the vectors defined in (9). The above equation can be written in non-conservative form as follows:

$$\boldsymbol{A}\frac{\mathrm{d}\boldsymbol{U}}{\mathrm{d}x} = \boldsymbol{S} \tag{24}$$

where $\boldsymbol{U}$ is the vector defined in (9) and $\boldsymbol{A}$ is the Jacobian matrix defined in (11). Let us consider the domain $\Omega = (0, L)$, $L \in \mathbb{R}^+$ bounded by Γ. Clearly,

$\Gamma = \Gamma_0 \cup \Gamma_L$ if we define Γ_0 as the point $x = 0$ and Γ_L as $x = L$. By using this notation the inflow boundary (which will be denoted by Γ^{in}) will be Γ_0 when $a > 0$ and Γ_L in the opposite case. The outflow boundary will be the complementary of the inflow one. Therefore, this problem can be stated as follows:

$$\boldsymbol{A}\frac{\mathrm{d}\boldsymbol{U}}{\mathrm{d}x} = \boldsymbol{S} \qquad \text{in} \quad \Omega \tag{25.1}$$

$$\boldsymbol{U}^{\text{in}} = \boldsymbol{U}_D^{\text{in}} \qquad \text{on} \quad \Gamma \tag{25.2}$$

where $\boldsymbol{U}^{\text{in}}$ represents the inflow components of $\boldsymbol{U}$. It is straightforward to write (25.1) as:

$$\frac{\mathrm{d}q}{\mathrm{d}x} = -a\frac{\mathrm{d}u}{\mathrm{d}x} \tag{26.1}$$

$$k\frac{\mathrm{d}u}{\mathrm{d}x} + \tau a\frac{\mathrm{d}q}{\mathrm{d}x} = -q \tag{26.2}$$

By introducing (26.1) into (26.2) it can be shown that

$$q = -(k - \tau a^2)\frac{\mathrm{d}u}{\mathrm{d}x} \tag{27}$$

If we use (26.1) and the derivative of (26.2), the following second order equation is found:

$$a\frac{\mathrm{d}u}{\mathrm{d}x} - (k - \tau a^2)\frac{\mathrm{d}^2u}{\mathrm{d}x^2} = 0 \tag{28}$$

Equation (28) shows clearly that Cattaneo's law introduces a negative diffusion with respect to Fick's law. It may be argued that this fact represents an important drawback of the hyperbolic model because it complicates the numerical resolution of the equation. However, we will see in the numerical examples that this is not the case.

It is very important to note that it has been necessary to derivate (26.2) in order to derive equation (28). Therefore, *spurious solutions could have been introduced in* (28). However, we can avoid to obtain spurious solutions by imposing to (28) the same boundary conditions which have been imposed to (25). In supercritical flow we should impose u and q on the inflow boundary. The boundary condition regarding q can be imposed by using the relation (27). We must not impose boundary conditions on the supercritical outflow boundary. In a subcritical problem one component of $\boldsymbol{U}$ (u for instance) should be prescribed on the inflow boundary and the other one (q in this case) should be imposed on the outflow boundary. However, it is also correct to prescribe concentration on Γ_0 and Γ_L in subcritical flow conditions because we are imposing one condition at each boundary.

4.2 The effect of the standard Galerkin discretization on the classic parabolic convection-diffusion equation

In this section we prove that (under the necessary assumptions) when a standard Galerkin discretization is applied to the classic parabolic convection-diffusion equation, the velocity of propagation is not infinite anymore. On the contrary, a finite velocity of propagation can be identified in the discrete equations. By means of a comparison with the hyperbolic model we conclude that the standard Galerkin formulation introduces an "artificial" relaxation time.

We will carry on this study by analyzing the classic parabolic convection-diffusion problem subjected to homogeneous Dirichlet boundary conditions. Therefore, we state the following problem: find a function $u\colon [0,L] \mapsto \mathbb{R}$ such that

$$a\frac{\mathrm{d}u}{\mathrm{d}x} - k\frac{\mathrm{d}^2u}{\mathrm{d}x^2} = 0; \quad x \in (0,L) \tag{29.1}$$

$$u(0) = u_0 \tag{29.2}$$

$$u(L) = u_L \tag{29.3}$$

Let $0 = x_0 < x_1 < \cdots < x_N = L$ be a uniform partition of the interval $[0,L]$. We call h the distance between two consecutive nodes. Let us call

$$P_{\mathsf{e}} = \frac{ah}{2k} \tag{30}$$

the *mesh Péclet number* which expresses the ratio of convective to diffusive transport. If we solve (29) by using the standard Galerkin method and linear finite elements we obtain the following discrete equation at an interior node j [25]:

$$(1-P_{\mathsf{e}})u_{j+1} - 2u_j + (1+P_{\mathsf{e}})u_{j-1} = 0 \tag{31}$$

In the above equation u_j is the finite element approximation of $u(x_j)$ and u_0, u_N are the values given by the boundary conditions of (29). In addition, difference equations (31) can be solved exactly (see, for instance, reference [26]) since they are linear equations. The exact solution of (31) (subject to boundary conditions (29.2) and (29.3)) is

$$u_j = \frac{1}{1-\left(\frac{1+P_{\mathsf{e}}}{1-P_{\mathsf{e}}}\right)^N}\left\{u_0\left[\left(\frac{1+P_{\mathsf{e}}}{1-P_{\mathsf{e}}}\right)^j - \left(\frac{1+P_{\mathsf{e}}}{1-P_{\mathsf{e}}}\right)^N\right] + u_L\left[1-\left(\frac{1+P_{\mathsf{e}}}{1-P_{\mathsf{e}}}\right)^j\right]\right\} \tag{32}$$

so oscillations will occur when $|P_{\mathsf{e}}| > 1$.

On the other hand, the exact solution of (29) is

$$u(x_j) = \frac{1}{1-e^{\frac{ah}{k}N}}\left[u_0\left(e^{\frac{ah}{k}j} - e^{\frac{ah}{k}N}\right) + u_L\left(1-e^{\frac{ah}{k}j}\right)\right] \tag{33}$$

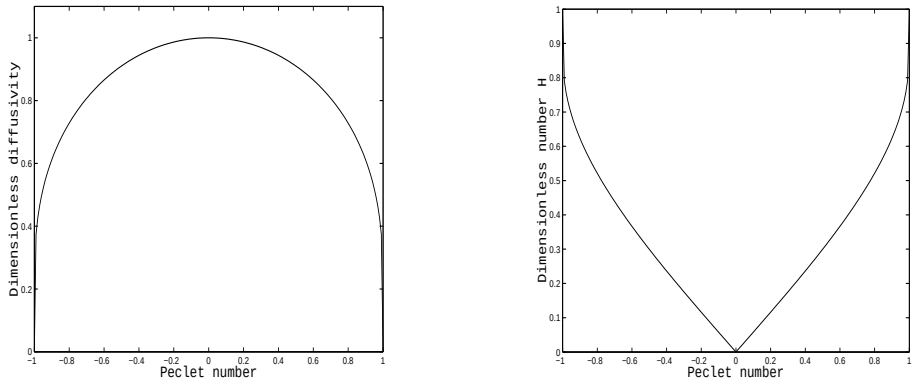

Fig. 1. Dimensionless diffusivity ($k^\star/k$) as a function of P_e (left) and dimensionless number H as a function of P_e (right).

A simple comparison between (32) and (33) shows that the approximate solution equals the exact one if the following relation holds

$$e^{2P_\mathsf{e}j} = \left(\frac{1+P_\mathsf{e}}{1-P_\mathsf{e}}\right)^j \quad \forall j = 0, \ldots, N \tag{34}$$

Relation (34) is only satisfied for $P_\mathsf{e} = 0$ (pure-diffusive problem). However, it can be shown that when $|P_\mathsf{e}| \leq 1$ (i.e. when the mesh is fine enough) the approximate solution (32) is, in fact, the exact solution of a Cattaneo-type problem for a certain relaxation time. To show the former assertion we will prove that (32) is the exact solution of the problem

$$a\frac{\mathrm{d}u}{\mathrm{d}x} - k^\star\frac{\mathrm{d}^2u}{\mathrm{d}x^2} = 0; \quad x \in (0, L) \tag{35.1}$$

$$u(0) = u_0 \tag{35.2}$$

$$u(L) = u_L \tag{35.3}$$

for a certain $k^\star \leq k$. To grant that (32) satisfies (35) the following relation must be fulfilled:

$$e^{\frac{ah}{k^\star}j} = \left(\frac{1+P_\mathsf{e}}{1-P_\mathsf{e}}\right)^j \quad \forall j = 0, \ldots, N \tag{36}$$

We want to obtain $k^\star$ such that (36) holds. If we admit complex solutions, then $k^\star$ can always be determined. If we exclusively admit $k^\star$ to be a real number, then (36) has a solution only when $|P_\mathsf{e}| \leq 1$. The solution of (36) is

$$k^\star = k\frac{2P_\mathsf{e}}{\ln\left(\frac{1+P_\mathsf{e}}{1-P_\mathsf{e}}\right)} \tag{37}$$

By means of (37) we notice that $k^\star \to 0$ as $|P_\mathsf{e}| \to 1$ and $k^\star \to k$ as $|P_\mathsf{e}| \to 0$. See figure 1 where $k^\star/k$ is represented for $P_\mathsf{e} \in (-1, 1)$. Therefore, the standard Galerkin method applied to (29) solves exactly an underdiffusive equation. On

the other hand, equation (37) can be rearranged as

$$k^\star = k - k\left(1 - \frac{2P_\mathsf{e}}{\ln\left(\frac{1+P_\mathsf{e}}{1-P_\mathsf{e}}\right)}\right) < k \tag{38}$$

If we compare the diffusive coefficient $k^\star$ with the coefficient which results of using Cattaneo's law (see equation (28)) the following conclusion is achieved: when we solve (29) by using the standard Galerkin method we obtain the solution of a Cattaneo-type transport problem defined by the following relaxation time:

$$\tau_G = \frac{h}{a}\left(\frac{1}{2P_\mathsf{e}} - \frac{1}{\ln\left(\frac{1+P_\mathsf{e}}{1-P_\mathsf{e}}\right)}\right) \tag{39}$$

Therefore, *an "artificial" relaxation time has been introduced by the Galerkin formulation* . As a result, *a finite velocity of propagation can be defined in the discrete equation* (31)*:*

$$c_G = \frac{a}{\left(1 - \frac{2P_\mathsf{e}}{\ln\left(\frac{1+P_\mathsf{e}}{1-P_\mathsf{e}}\right)}\right)^{1/2}} \tag{40}$$

By using the relation (40) it is easy to compute the value of "artificial" H (the dimensionless number defined in (19)) for a certain P_e. In figure 1 it has been represented the "artificial" H as a function of P_e. As a result, when we solve the problem (29) for $|P_\mathsf{e}| < 1$ by using the standard Galerkin method we are really solving a Cattaneo-type transport problem in subcritical flow conditions. Therefore, we solve a well posed problem because boundary conditions (29.2), (29.3) can be imposed in subcritical flow. However, as $|P_\mathsf{e}| \to 1$ the problem which is really solved tends to an ill-posed problem.

In what follows we will solve numerically the steady state Cattaneo-type transport equation in subcritical and supercritical flow conditions. In order to make easier the comparison between the Cattaneo-type transport and the standard formulation of the transport problem we will use equation (28) to describe the proposed model. However, we must take into account that boundary conditions that must be imposed are (25.2).

4.3 The standard Galerkin discretization of the hyperbolic model

In this section we will analyze the problem

$$a\frac{\mathrm{d}u}{\mathrm{d}x} - (k - \tau a^2)\frac{\mathrm{d}^2u}{\mathrm{d}x^2} = 0; \quad x \in (0, L) \tag{41.1}$$

$$u(0) = u_0 \tag{41.2}$$

$$u(L) = u_L \tag{41.3}$$

which represents a Cattaneo-type transport problem only in subcritical flow. Let us consider again the partition of $[0, L]$ defined by the nodes $0 = x_0 < x_1 < \cdots < x_N = L$. We call $h = L/N$.

At this point it is useful to define the dimensionless number

$$H_{\mathsf{e}} = \frac{ah}{2(k - \tau a^2)} \tag{42}$$

which plays a similar role to P_{e} in the standard description of the transport problem [13,14]. If we solve (41) by using the standard Galerkin method and linear finite elements, the following difference equations are found [12]:

$$(1 - H_{\mathsf{e}})u_{j+1} - 2u_j + (1 + H_{\mathsf{e}})u_{j-1} = 0; \quad \forall j = 1, \ldots, N-1 \tag{43}$$

where u_0 and u_N are given by the boundary conditions (41.2) and (41.3). In the same way as (31), difference equations (43) can be solved exactly and the stability condition

$$|H_{\mathsf{e}}| \leq 1 \tag{44}$$

can be found. If we take $\tau = 0$ in (44) we obtain

$$|P_{\mathsf{e}}| \leq 1 \tag{45}$$

which constitutes a stability condition for the standard formulation. Relations (44) and (45) seem not to be very useful because they can only be applied to (41.1) and (29.1), respectively. However, the asymptotic behavior of (44) is equivalent (except for a scale factor) to impose that the grid step size is smaller than typical sizes related to the waves which give the solution of the Cattaneo-type transport problem. As we said before, the waves which determine the solution propagate with celerities $a - c$ and $a + c$. Thus, typical sizes upstream and downstream are $\tau(c - a)$ and $\tau(a + c)$, respectively. Hence, it is possible to show [12] that

$$h < \min\left(\tau(c - a), \tau(a + c)\right) \tag{46}$$

tends to (44) as a tends to the mass wave celerity c, except for a scale factor.

In what follows we will present some numerical solutions of the hyperbolic convection-diffusion model. For all the examples in section 4 we use a 20 (linear) element discretization, $L = 1$ (thus, $h = 0.05$) and $k = 1$.

4.4 Numerical examples in subcritical flow

Now we represent the approximate solution and the exact solution of the hyperbolic convection-diffusion problem. Two groups of numerical examples will be presented. At each group the relaxation time is a constant. As we said

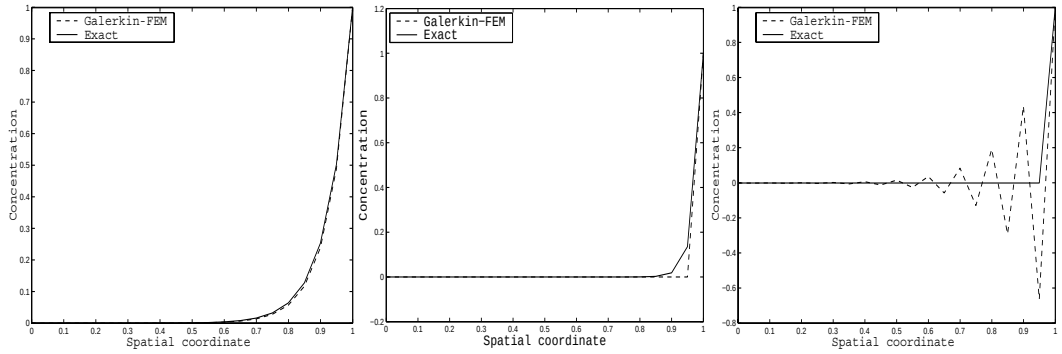

Fig. 2. Three subcritical transport problems by using Cattaneo's law. These problems are defined by $k = 1$, $\tau = 0.01$ and three different H values: $H = 0.7$ (left), $H = 0.8828$ (center), $H = 0.975$ (right). Numerical solutions are obtained by using the Galerkin FEM with linear shape functions. A 20 element grid has been used.

before, we use a 20 (linear) element mesh, $L = 1$ (thus, $h = 0.05$) and $k = 1$ for all examples in section 4. However, at each group we will show three results defined by different fluid velocity values.

4.4.1 Group 1: small relaxation time

This first group of results is defined by $\tau = 0.01$. By using the above values for k and τ we obtain the diffusive wave celerity $c = \sqrt{k/\tau} = 10$. Thus, if $|a| \geq 10$, then (41) does not represent a Cattaneo-type transport problem anymore. Our next step will be calculate the maximum a value to obtain a stable solution of (41) by using the stability condition $|H_{\mathsf{e}}| \leq 1$. If we do that we will see that the numerical scheme used will yield stable solutions when $|a| \leq 8.8278$. Therefore, we can say that the numerical solution of (41) is stable for an important range of the possible values of a, because (41) does not represent a Cattaneo-type transport problem when $|a| \geq 10$.

In figure 2 we show the numerical (dashed line) and the exact (solid line) solutions for three a values. On the left, solutions for $a = 7$ are plotted. The middle graphic shows solutions for $a = 8.8278$ which is the largest a value that entails a stable numerical solution. Finally, we plot solutions for $a = 9.75$ on the right.

4.4.2 Group 2: medium relaxation time

This group of problems is defined by $\tau = 1$. Therefore, the mass wave celerity is $c = \sqrt{k/\tau} = 1$. In addition, according to the stability condition (44), the largest velocity that entails a stable solution is $a = 0.9876$. Hence, we will obtain stable solutions if $|a| \leq 0.9876$, that is, for almost all possible values of a because if $|a| \geq 1$, then (41) does not represent a Cattaneo-type transport

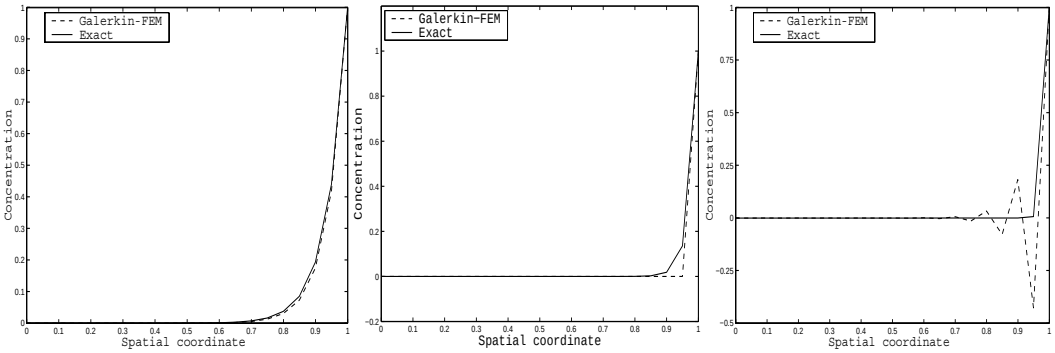

Fig. 3. Three subcritical transport problems by using Cattaneo's law. These problems are defined by $k = 1$, $\tau = 1$ and three different H values: $H = 0.97$ (left), $H = 0.9876$ (center), $H = 0.995$ (right). Numerical solutions are obtained by using the Galerkin FEM with linear shape functions. A 20 element grid has been used.

problem anymore. We show three numerical tests for this relaxation time in figure 3. Solutions for $a = 0.97$ (left), $a = 0.9876$ (center) and $a = 0.995$ (right) are plotted.

4.5 Numerical examples in supercritical flow

In this section, some numerical solutions of the Cattaneo-type transport problem in supercritical flow are presented. As we said above, in supercritical flow u and q must be prescribed on the inflow boundary. Boundary conditions involving the flux q will be imposed weakly by using (27). There is no restriction in supposing $a > 0$. In this way, we can determine the inflow boundary which is Γ_0. Accordingly, we will analyze the problem

$$a\frac{\mathrm{d}u}{\mathrm{d}x} - (k - \tau a^2)\frac{\mathrm{d}^2 u}{\mathrm{d}x^2} = 0; \quad x \in (0, L) \tag{47.1}$$

$$u(0) = u_0 \tag{47.2}$$

$$\frac{\mathrm{d}u}{\mathrm{d}x}(0) = -\frac{q_0}{k - \tau a^2} \tag{47.3}$$

which could also be analyzed by solving system (26) provided with boundary conditions $u(0) = u_0$, $q(0) = q_0$. However, we analyze the Cattaneo-type transport problem by solving (47) in order to be consistent with the previous section. In the same way as in section 4.4, two groups of numerical examples will be presented. At each group the relaxation time is a constant. The values of L, k and h are the same as in the previous section. The boundary values ($u_0 = 1$ and $q_0 = -1$) are the same for all the numerical tests.

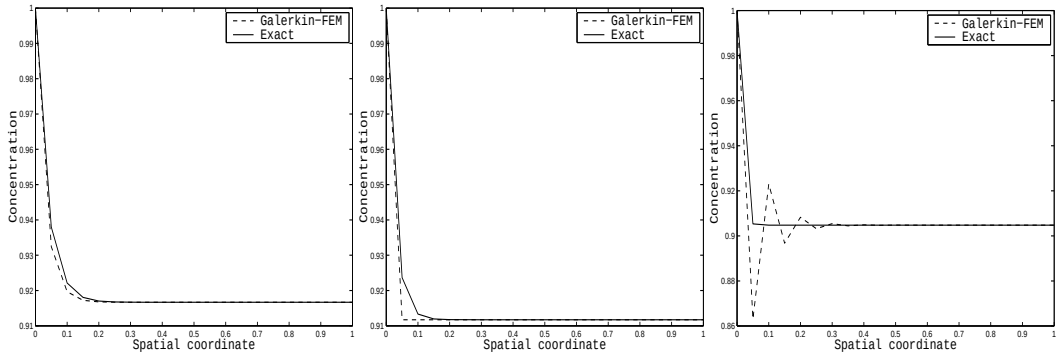

Fig. 4. Three supercritical transport problems by using Cattaneo's law. These problems are defined by $k = 1$, $\tau = 0.01$ and three different H values: $H = 1.2$ (left), $H = 1.1328$ (center), $H = 1.05$ (right). Numerical solutions are obtained by using the Galerkin FEM with linear shape functions. A 20 element grid has been used.

4.5.1 Group 1: small relaxation time

This first group is defined by $\tau = 0.01$. It is straightforward to compute $c = \sqrt{k/\tau} = 10$. It has already been said that (47) represents a Cattaneo-type transport problem when $|a| > 10$. The minimum a value to obtain a stable solution is given by the condition $|H_{\mathsf{e}}| \leq 1$. Making some algebra in the above relation we conclude that stable solutions will be obtained when $|a| \geq 11.3278$. Therefore, we can say that the numerical solution of (47) is stable for an important range of the possible a values.

In figure 4 we show the numerical (dashed line) and exact (solid line) solutions for three a values. On the left, solutions for $a = 12$ are plotted. The middle graphic shows solutions for $a = 11.3278$ which is the minimum a value that entails a stable numerical solution. Finally, we plot solutions for $a = 10.5$ on the right.

4.5.2 Group 2: medium relaxation time

This group is defined by the relaxation time $\tau = 1$. Therefore, the mass wave celerity is $c = 1$. We show three numerical tests for this relaxation time in figure 5. Solutions for $a = 1.05$ are plotted on the left. The middle graphic shows solutions for $a = 1.0126$ which is the minimum a value that yields a stable solution. Finally, we plot solutions for $a = 1.005$ on the right.

4.6 Conclusions from the numerical examples

From the previous numerical examples we conclude that in the hyperbolic model numerical instabilities do not arise for large values of the fluid velocity a, but they appear for values of $|a|$ close to the pollutant velocity c.

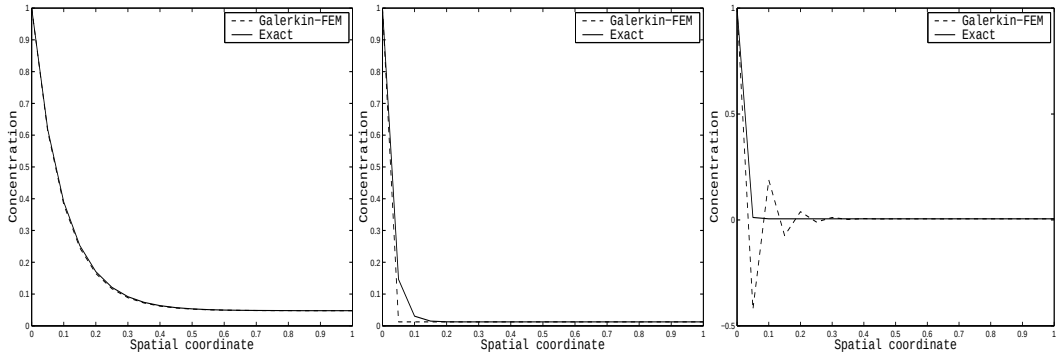

Fig. 5. Three supercritical transport problems by using Cattaneo's law. These problems are defined by $k = 1$, $\tau = 1$ and three different H values: $H = 1.05$ (left), $H = 1.0126$ (center), $H = 1.005$ (right). Numerical solutions are obtained by using the Galerkin FEM with linear shape functions. A 20 element grid has been used.

In addition, we have shown that if we use Cattaneo's law we obtain stable solutions in a very significative part of the domain of a. This is true even if we use the standard Galerkin method. Further, we can conclude that *as τ increases transport problem becomes more stable*. Indeed, it can be proved that the size (in the velocity domain) of the interval that leads to unstable solutions is

$$I = h/\tau \tag{48}$$

which decreases as τ increases. In order to prove the above assertion we will find the a values that make

$$|H_{\mathsf{e}}| = 1 \tag{49}$$

It is easy to prove that (49) possesses 4 real solutions, namely

$$a_1 = -\frac{h}{4\tau} - \sqrt{\left(\frac{h}{4\tau}\right)^2 + c^2} \tag{50.1}$$

$$a_2 = -\frac{h}{4\tau} + \sqrt{\left(\frac{h}{4\tau}\right)^2 + c^2} \tag{50.2}$$

$$a_3 = -a_2 \tag{50.3}$$

$$a_4 = -a_1 \tag{50.4}$$

Further, it is straightforward that $a_1 < 0$, $a_1 < -c$, $a_2 > 0$, $a_2 < c$. Taking into account all of this, the interval of velocities that makes the numerical solution unstable has a size of

$$I = a_4 - a_2 + a_3 - a_1 = -2(a_1 + a_2) = h/\tau \tag{51}$$

as we said above.

5 An application example: simulation of an accidental spillage in the port of A Coruña

The objective of this section is to investigate the possibilities of the hyperbolic model for real computations in engineering. We are interested in practical applications in civil and environmental engineering. For this reason, we present an example concerning the evolution of an accidental spillage in the harbor of A Coruña (northwest of SPAIN, EU).

5.1 Numerical algorithm

We will use the second order Taylor-Galerkin method to compute the numerical solution [27–29]. The details of the algorithm can be found in [1]. In this paper we only present the vectorial equation that must be solved at each interior node B and at each time step

$$\sum_A M_{BA} \Delta \boldsymbol{U}_A^n = \boldsymbol{f}_B^n \tag{52}$$

where

$$M_{BA} = \iint_\Omega N_B N_A \mathrm{d}\Omega \tag{53.1}$$

$$\boldsymbol{f}_B^n = \iint_\Omega N_B \boldsymbol{b}^n \mathrm{d}\Omega + \iint_\Omega \boldsymbol{G}^n \nabla_{\boldsymbol{x}} (N_B) \mathrm{d}\Omega - \int_\Gamma N_B \boldsymbol{G}^n \boldsymbol{n} \mathrm{d}\Gamma \tag{53.2}$$

$$\boldsymbol{b}^n = \Delta t \boldsymbol{S}^n + \frac{\Delta t^2}{2} \boldsymbol{B} \boldsymbol{S}^n \tag{53.3}$$

$$\boldsymbol{G}^n = \Delta t \boldsymbol{F}^n + \frac{\Delta t^2}{2} \boldsymbol{B} \boldsymbol{F}^n - \frac{\Delta t^2}{2} \boldsymbol{P}^n \tag{53.4}$$

being N_A, N_B linear interpolating functions, $\boldsymbol{B} = \nabla_{\boldsymbol{U}} (\boldsymbol{S})$ and $\boldsymbol{P}$ the matrix that results of assembling the following vectors:

$$\boldsymbol{P}_i = -\boldsymbol{A}_i (\boldsymbol{S} - \nabla_{\boldsymbol{x}} \cdot (\boldsymbol{F})); \quad i = 1, 2 \tag{54}$$

$\boldsymbol{U}$, $\boldsymbol{F}$ and $\boldsymbol{S}$ have been defined in (22).

The mass matrix defined in (53.1) has been computed by using nodal integration which leads to a *lumped mass matrix* [30]. The integrals appearing in the rest of the terms have been approximated by means of a 2×2 points Gauss-Legendre quadrature. The boundary terms have been integrated by using a 2 points Gauss-Legendre formula.

Fig. 6. Simulation of an accidental spillage in the port of A Coruña. Digital photograph showing the port.

5.2 Problem setup

The domain of the problem comprises the whole area of the A Coruña port. In figure 6 we show a digital photograph of the port. We represent the layout of the port in figure 7. To bound the domain of the problem we define an open sea boundary from the end of Barrie's dike to the extreme of Oza's dock. The resulting computational domain has been depicted in figure 8 (left). As it can be seen in this figure some elements of the real domain have been removed in order to simplify the generation of the mesh. However, the omission of these elements is not important for the solution of the problem [32]. For instance, the oil tanker pier allows both water and pollutant to flow through it, so it does not modify the solution.

Three kinds of boundaries are differentiated in figure 8 (left): the solid wall boundary has been plotted in green; the boundary where the spillage happens has been plotted in red; the open sea boundary has been plotted in blue.

The objective of this example is to show that the proposed methodology can be used to simulate real engineering problems. For this reason we have not considered necessary to perform an accurate estimation of the parameters which would entail a lot of experimental work. A typical value for engineering calculations has been selected for the diffusivity k [33]. The estimation of the relaxation time τ is not so trivial since only the order of magnitude of

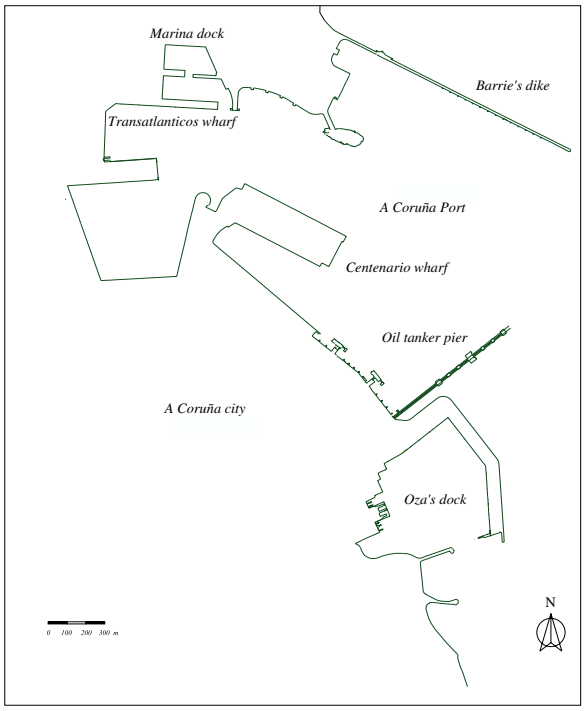

Fig. 7. Simulation of an accidental spillage in the port of A Coruña. Layout of the port.

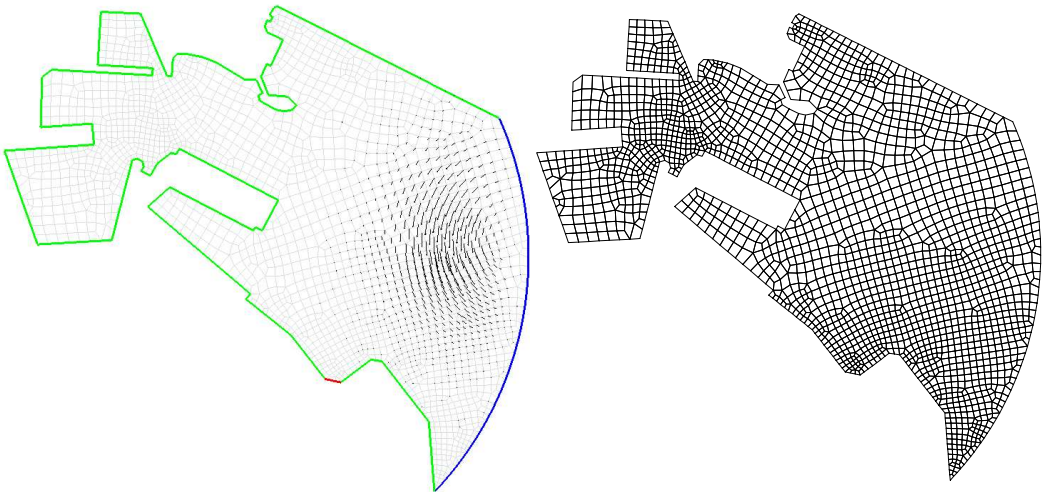

Fig. 8. Simulation of an accidental spillage in the port of A Coruña. Velocity field and kinds of boundaries (left) and computational mesh of the problem (right). On the left hand side the solid wall boundary has been plotted in green; the boundary where the spillage happens has been plotted in red; the open sea boundary has been plotted in blue. The finite element mesh consists of 2023 bilinear elements and it was generated by using the code GEN4U [31].

the parameter can be estimated without making experiments. However, what really determines the solution is the velocity of the fluid $\boldsymbol{a}$ with respect to the velocity of the pollutant $c = \sqrt{k/\tau}$. This quotient defines a Mach-type number as it can be seen in equation (19).

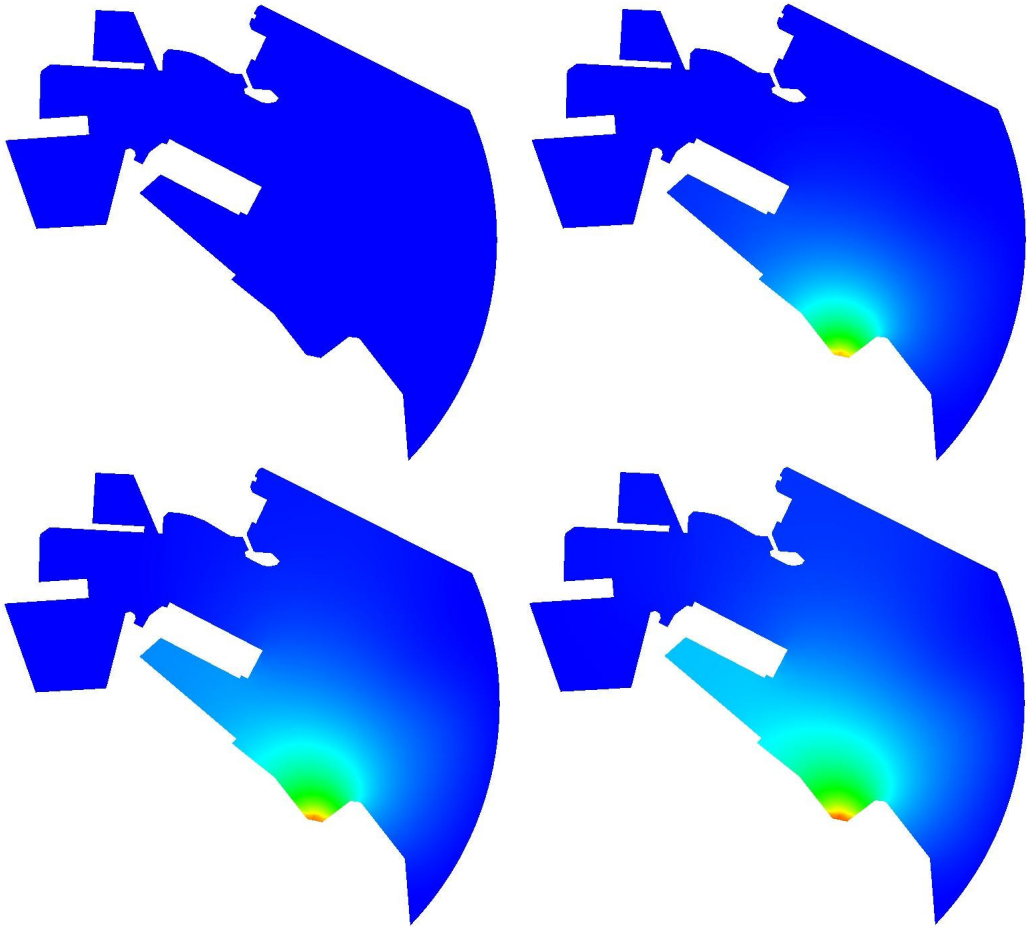

Fig. 9. Simulation of an accidental spillage in the port of A Coruña. We show (left to right and top to bottom) the concentration initial condition and concentration solutions at non-dimensional times $t^* = 30$, $t^* = 60$ and $t^* = 90$.

In order to reduce the computations, the velocity field has not been calculated, but it was generated with two constraints: a) it verifies the continuity equation for incompressible flow and b) it satisfies standard boundary conditions for a viscous flow. The velocity field has been plotted in figure 8 (left). On the right hand side of figure 8 we have depicted the computational mesh.

On the solid wall boundary we impose $\boldsymbol{q} \cdot \boldsymbol{n} = 0$. On the boundary where the spillage takes place the condition $\boldsymbol{q} \cdot \boldsymbol{n} = -10^{-2}$ is imposed. On the open sea boundary we impose $\boldsymbol{q} \cdot \boldsymbol{n} = cu$ where $c = \sqrt{k/\tau}$ is the pollutant wave velocity. The flow is given by H numbers ($H = ||\boldsymbol{a}||/c$) verifying $H \leq H_{\max} \approx 0.3237$ what makes the problem to be subcritical at each point of the domain. The computation was performed taking a maximum CFL number $C_{\max} \approx 0.5531$.

At this point we define the non-dimensional time $t^* = t/\tau$. In figure 9 we show the initial concentration and concentration solutions at non-dimensional times $t^* = 30$, $t^* = 60$ and $t^* = 90$. In figure 10 concentration solutions at non-dimensional times $t^* = 120$, $t^* = 150$, $t^* = 300$ and $t^* = 1000$ are plotted.

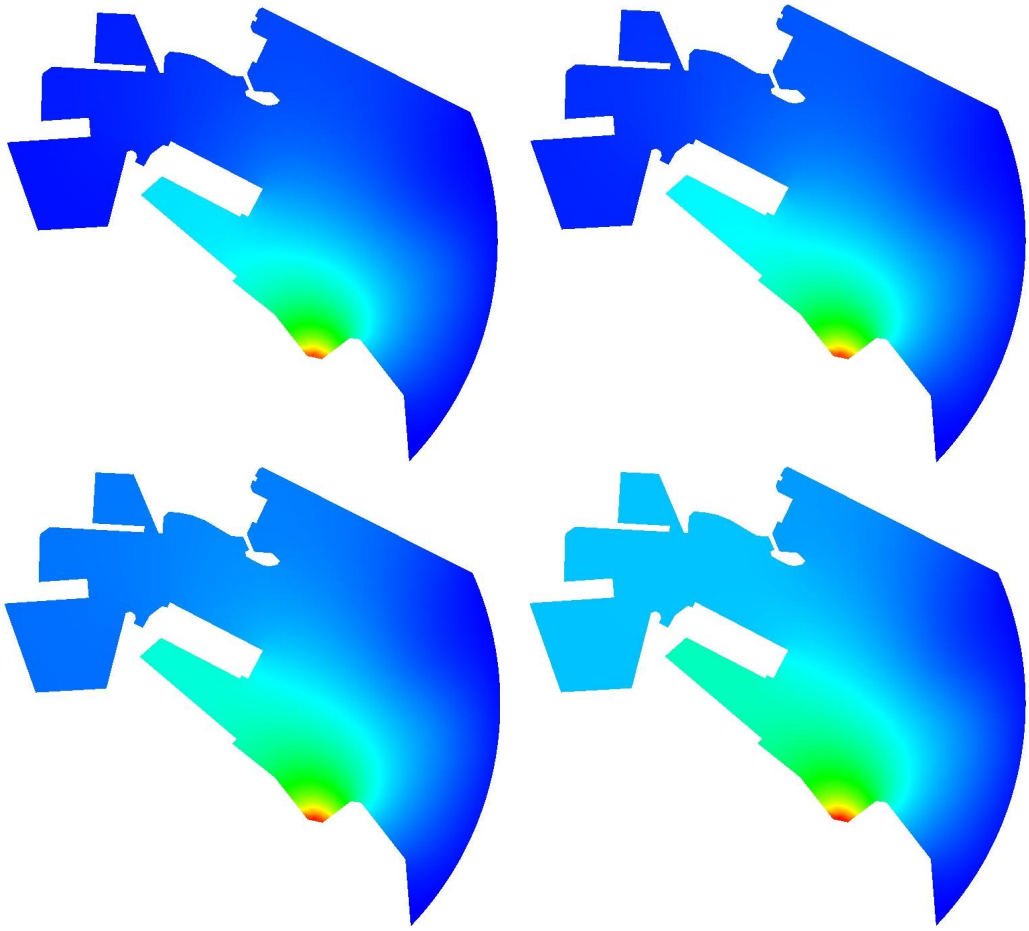

Fig. 10. Simulation of an accidental spillage in the port of A Coruña. We show (left to right and top to bottom) concentration solutions at non-dimensional times $t^* = 120$, $t^* = 150$, $t^* = 300$ and $t^* = 1000$.

6 Conclusions and future developments

In this paper, a hyperbolic model for convection-diffusion problems in CFD is analyzed. The hyperbolic formulation avoids the infinite speed paradox inherent to the standard parabolic formulation. The proposed formulation constitutes a generalized approach for convective-diffusive phenomena because the standard formulation can be considered as a subcase of the proposed one.

From a numerical point of view, we have shown that the discrete equations of the Fick-type 1D steady model represent, in fact, a Cattaneo-type transport when the standard Galerkin formulation is employed. In addition, we show that the Galerkin solution (with linear elements) of the proposed equations is stable for any value of the fluid velocity except for a small interval whose length decreases as the relaxation time increases.

Finally, we present an application in environmental engineering in order to

explore the possibilities of the hyperbolic model for real computations. We conclude that the proposed model is a feasible alternative to the standard parabolic models. However, there are some issues that should be addressed: for example those concerning the computational cost of the numerical approach and the estimation of the parameters of the model (especially the relaxation time τ).

7 Acknowledgements

This work has been partially supported by Grant Numbers PGIDT03PXIC18001PN and PGIDT05PXIC18002PN of the "Subdirección Xeral de I+D de la Xunta de Galicia", by Grant Numbers DPI2002-00297 and DPI2004-05156 of the "Ministerio de Educación y Ciencia", and by research fellowships of the "Universidade da Coruña" and the "Fundación de la Ingeniería Civil de Galicia".

References

[1] H. Gómez, I. Colominas, F. Navarrina, M. Casteleiro, A finite element formulation for a convection-diffusion equation based on Cattaneo's law, Computer Methods in Applied Mechanics in Engineering, (2006), in press.

[2] A. Compte, The generalized Cattaneo equation for the description of anomalous transport processes, Journal of Physics A: Mathematical and General, **30** (1997) 7277–7289.

[3] M.N. Özisik, D.Y. Tzou, On the wave theory in heat conduction, ASME J. Heat Transf., **116** (1994) 526–535.

[4] A. Fick, Uber diffusion, Poggendorff's Annalen der Physik und Chemie, **94** (1855) 59–86.

[5] J.B. Fourier, Théorie analytique de la chaleur, Jacques Gabay, 1822.

[6] M.C. Cattaneo, Sur une forme de l'equation de la chaleur liminant le paradoxe d'une propagation instantane, Comptes Rendus de L'Academie des Sciences: Series I-Mathematics, **247** (1958) 431–433.

[7] B. Vick, M.N. Özisik, Growth and decay of a thermal pulse predicted by the hyperbolic heat conduction equation, ASME Journal of Heat Transfer, **105** (1983) 902–907.

[8] Joseph, D.D., Preziosi, L., Heat waves, Reviews of Modern Physics, **61** (1989) 41–73.

[9] Joseph, D.D., Preziosi, L., Addendum to the paper "Heat waves", Reviews of Modern Physics, **62** (1990) 375–391.

[10] M. Zakari, D. Jou, Equations of state and transport equations in viscous cosmological models, Physical Review D, **48** (1993) 1597–1601.

[11] T. Ruggeri, A. Muracchini, L. Seccia, Shock waves and second sound in a rigid heat conductor: A critical temperature for NaF and Bi, Physical Review Letters, **64** (1990) 2640–2643.

[12] H. Gómez, A new formulation for the advective-diffusive transport problem, Technical Report (in Spanish), University of A Coruña, 2003.

[13] H. Gómez, I. Colominas, F. Navarrina, M. Casteleiro, An alternative formulation for the advective-diffusive transport problem, 7^{th} Congress on Computational Methods in Engineering, eds. C.A. Mota Soares, A.L. Batista, G. Bugeda, M. Casteleiro, J.M. Goicolea, J.A.C. Martins, C.A.B. Pina, H.C. Rodrigues, Lisbon, Portugal, 2004.

[14] H. Gómez, I. Colominas, F. Navarrina, M. Casteleiro, On the intrinsic instability of the advection–diffusion equation, Proc. of the 4^{th} European Congress on Computational Methods in Applied Sciences and Engineering (CDROM), eds. P. Neittaanmäki, T. Rossi, S. Korotov, E. Oñate, J. Priaux y D. Knörzer, Jyväskylä, Finland, 2004.

[15] M. Arora, Explicit characteristic-based high resolution algorithms for hyperbolic conservation laws with stiff source terms, Ph.D. dissertation, University of Michigan, 1996.

[16] G.F. Carey, M. Tsai, Hyperbolic heat transfer with reflection, Numerical Heat Transfer, **5** (1982) 309–327.

[17] H.Q. Yang, Solution of two-dimensional hyperbolic heat conduction by high resolution numerical methods, AIAA-922937 (1992).

[18] M.T. Manzari, M.T. Manzari, On numerical solution of hyperbolic heat equation, Communications in Numerical Methods in Engineering, **15** (1999) 853–866.

[19] Christov, C.I., Jordan, P.M., Heat conduction paradox involving second-sound propagation in moving media, Physical Review Letters, **94** (2005) 4301-4304.

[20] R. Courant, D. Hilbert, Methods of mathematical physics. Vol II., John Wiley & Sons, 1989.

[21] R. Courant, K.O. Friedrichs, Supersonic flow and shock waves, Springer Verlag, 1999.

[22] G.B. Whitham, Linear and nonlinear waves, John Wiley & Sons, 1999.

[23] F. Alcrudo, Total variation diminishing high-resolution schemes for free surface flows, PhD dissertation (in Spanish), University of Zaragoza, 1992.

[24] H. Gómez, A hyperbolic formulation for convective-diffusive problems in CFD, Ph.D. dissertation (in Spanish), University of A Coruña, 2006.

[25] R. Codina, A finite element formulation for the numerical solution of the convection-diffusion equation, Technical Report 14, International Center for Numerical Methods in Engineering (CIMNE), 1993.

[26] E. Isaacson, H.B. Keller, Analysis of numerical methods, John Wiley & Sons, 1966.

[27] J. Donea, A Taylor-Galerkin method for convective transport problems, International Journal for Numerical Methods in Engineering, **20** (1984) 101–120.

[28] J. Donea, L. Quartapelle, V. Selmin, An analysis of time discretization in the finite element solution of hyperbolic problems, Journal of Computational Physics, **70** (1987) 463–499.

[29] J. Donea, L. Quartapelle, An introduction to finite element methods for transient advection problems, Computer Methods in Applied Mechanics and Engineering, **95** (1992) 169–203.

[30] T.J.R. Hughes, The finite element method. Linear static and dynamic finite element analysis, Dover Publications, 2000.

[31] J. Sarrate, A. Huerta, Efficient unstructured quadrilateral mesh generation, International Journal for Numerical Methods in Engineering, **49** (2000) 1327–1350.

[32] C.A. Figueroa, I. Colominas, G. Mosqueira, F. Navarrina, M. Casteleiro, A stabilized finite element approach for advective-diffusive transport problems, Proceedings of the XX Iberian Latin-American Congress on Computational Methods in Engineering (CDROM), eds. P.M. Pimenta, R.Brasil, E.Almeida, São Paulo, Brasil, 1999.

[33] E.R. Holley, Diffusion and Dispersion, Environmental Hydraulics, 111-151, V.P. Singh and W.H. Hager (Eds.), Kluwer: Dordrecht, 1996.